Journal of Smart Systems and Stable Energy, 1(4): 319-332 Autumn 2022

ORIGINAL RESEARCH PAPER

Developing Hierarchical RBF Neural Network for Model Identification of SOFCs using a Developed Coronavirus Herd Immunity Algorithm

Antonella Pasternak[1] and Charis Bresser[2]

1. College of Engineering, University of Miami, Coral Gables, FL 33146, USA
2. Department of Electrical Engineering, University of North Texas, USA

Received: 2021-04-18 Accepted: 2021-09-11 Published: 2022-10-01

ABSTRACT

A new Blackbox technique has been presented in the current paper for model estimation of the solid oxide fuel cells (SOFCs) for providing better results. The proposed method is based on a Hierarchical Radial Basis Function (HRBF). The presented method is then developed by a new modified metaheuristic, called Developed Coronavirus Herd Immunity Algorithm. The suggested model has been named DCHIA-HRBF. The proposed model is then trained by some data and prepared for the identification and prediction. The model is then analyzed and were put in comparison with several latest techniques for validation of the efficiency of the technique. It is also verified by the empirical data to prove its validation with the real data. Simulation results specified that the suggested DCHIA-HRBF delivers high effectiveness as an identifier and prediction tool for the SOFCs.

Keywords: *Solid Oxide Fuel Cell; hierarchical RBF neural network; Developed Coronavirus Herd Immunity Algorithm; model identification*

How to cite this article
FAMILY N. Developing Hierarchical RBF Neural Network for Model Identification of SOFCs using a Developed Coronavirus Herd Immunity Algorithm. Journal of Smart Systems and Stable Energy, 2022; 1(4): 319-332.
DOI: 10.52293/SE.1.1.319332

1. INTRODUCTION

The fossil fuels utilization as a long-lasting energy resource is hardly justified [1]. In particular, emissions of greenhouse gasses, carbon dioxide, and nitrous oxides are considered to be main reasons for global warming [2, 3]. Moreover, the fast population growth of the world causes the requirement for energy a necessary resource. It is estimated that this type of energy feeds nearly entire transportation and about 2/3 of electrical power [4]. In addition, these sources are not renewable and will run out one day [5, 6]. Examining the use of sustainable and renewable alternative sources is crucial and can meet needs of human [7]. Hence, work with different types of fuel cells (FC) as a new kind of sustainable sources of energy, due to its stability and safe and clean consumption, has increased [8].

* Corresponding Author Email: *pasternakantonella@gmail.com*

An advantage of fuel cells is proper electric effectiveness and fuel permeability of them. Reactions that are electrochemical are optimal and are carried out by supplying hydrogen and oxygen (air molecules) [9]. Consequently, H_2 oxidation fuel can be obtained with great efficiency [10]. The most significant element that affects the efficiency of the fuel cell is the catalyst [11]. Catalysts accelerate reactions at the positive and negative electrodes [12]. According to the electrolyte nature they can be classified into various types [13]. For various utilizations, specific fuels and materials are needed [14]. several fuel cells have been introduced. For example, Molten Carbonate Fuel Cell (MCFC), PEMFC, Alkaline Fuel Cell (AFC), Direct Methanol Fuel Cell (DMFC), Fosderic Acid Fuel Cell (PAFC), and Solid Oxide Fuel Cell (SOFC). Today, many researchers have focused

on building and improving solid oxide fuel cells [15]. SOFCs are beneficial widely due to electrical effectiveness of them, using gas potentiality, CH4 or biogas as fuel [16]. Different studies have pointed out the importance of fuel cells due to the lack of environmental pollution and the lack of noise and high efficiency [17]. Solid oxide fuel cell includes the cathode and the anode side, split by a component with high density like electrolytes such as gallium and zirconium [18]. Although many different approaches are developed for proper SOFCs model recently, it is challengeable yet [19]. Hence, it has been tried to deal with these challenges by combining and designing new techniques which may lead to an optimal design of the solid oxide fuel cells [20].

Xiong et al. [21] the SOFC system performance by identifying effective parameters through a simple competitive congestion metaheuristic technique. The optimization way with two solutions includes a simple learning equation and the new method of stochastic numbers which can solve voltage simulation problem. To assess the results of the suggested stochastic procedure of optimization, the Siemens energy cylindrical stack and the 5-kW dynamic tube cell were used. The dynamic behavior of the SOFC model was simulated with the help of precise identification of effective parameters through random metaheuristic procedures. The results showed that the optimized SOFC has more accuracy and reliability compared to other stochastic optimization algorithms.

Alhumade et al. [22] estimated the efficient parameters of SOFC through modern metaheuristic techniques. In the present study, the Equilibrium Optimization (EO) technique was used to find the effective system parameters to achieve the best simulation. To assess the efficiency of the optimized system, the simulated values were put in comparison with the actual voltage, and the accuracy of the simulation was measured using the Sum of Mean Squared Error (SMSE) criterion. The model was analyzed in both fixed and dynamic positions. The results of random optimization technique were put in comparison with several optimization methods like Archimedes Optimizer (AO), Student Psychology-based Optimizer (SPBO), Seagull Optimizer (SO), Marine Predator optimizer (MPO). The results of the output voltage simulation by optimization technique showed that the EO technique has a minimum SMSE (1.0406), so the results showed the superiority of EO for SOFC optimization.

Yang et al. [23] found the SOFC parameters using the extreme learning machine-based random optimization technique. Since the best way to control the optimal simulation of the output voltage is to find the effective parameters of the SOFC. In the present study, they used the optimization method to accurately simulate the voltage across the SOFC. To apply the proposed method, a 5 kW SOFC was used. The simulation results of the optimized model showed that the optimization technique has a high ability to simulate voltage. Because by accurately identifying the effective parameters of the system and increasing the speed in the simulation, it increases the efficiency of the system in energy production.

Ba et al. [24] analyzed the optimal Hopfield rotor Neural Network (RHNN) to evaluate the performance of SOFC model. Their innovation was to represent an optimized hybrid model which includes the RHNN model and the Gray Wolf Optimization algorithm (GWOA) to recognize the SOFC system efficiency. The Mean Square Error (MSE) was used to evaluate the proposed combined method. The proposed combined method was put in comparison with other popular technique consequences. The comparison achievements indicated that the optimized RHNN approach has a minimum error value. Moreover, the system optimized can calculate complex calculations in less time.

Jia et al. [25] evaluated the performance of SOFC by identifying unknown parameters using the Elman Neural Network (ENN) and Quantum Pathfinder (QPF) technique. The aim was to accurately simulate the output voltage of the system. To achieve the minimum MSE value between simulated voltage, and empirical voltage, the optimal ENN technique was performed in the SOFC system. The simulated values showed that the QPF-Elman model with 0.0014 MSE values, GWO-RHNN with 0.0017 MSE value, and PF-Elman with 0.0018 MSE value can simulate the voltage. The results using the obtained values showed that the QPF-Elman model has the most suitable simulation with a minimum angle.

However, the models introduced in the literature help investigate and optimize the solid oxide fuel cell, they face some limitations. Some models are based on different thermodynamic and mathematical laws, which are complex to be used in the applications. Therefore, using the experimental modeling can be so efficient and feasible for the

SOFC, with no information of the internal details. Hierarchical Radial Basis Function networks (HRBF) contains several RBF networks which are accumulated in cascade architecture to divide and solve it in multiple steps. Until now, there is no research work about using HRBF in modeling the solid oxide fuel cells.

In this study, the fuel utilization has been considered for modeling of the stacks. The main purpose is to use a radial basis function (RBF)-based artificial neural network (ANN) to provide a new Blackbox model identifier. In this paper, the HRBF network has been designed for modeling of the SOFC stack. Here, the hierarchical structure is also improved using a new improved metaheuristic algorithm to provide an SOFC model with higher efficiency.

2. THE FUNCTIONAL SOFC

The operational SOFC depends mostly on the transport system by using hydrogen and oxygen in reactions that are electrochemical. The conversion of the fuel's chemical energy and its oxidation into electricity is provided via the charge over 3 major elements [26]. A cathode and an anode is consisted in a dense electrolyte the main function of which is based on the results of oxygen-carrying charge ions (O_{2-}) from the division of air into oxygen ions and electrons [27]. Consequently, the generated ions from the dense electrolyte are taken to be stabilized with hydrogen at free electrodes and anodes [28]. The electrical power generated through the freed electrons moves to an exterior circuit by the outside bath. The main reactions of a SOFC are based on hydrogen-fed anode, oxygen-fed cathode and the whole transfer process, which are explicitly defined in subsequent models as follow [26]:

$$H_2 + O^{2-} \rightarrow H_2O + 2e^- \tag{1}$$

$$\frac{1}{2}O_2 + 2e^- \rightarrow O^{2-} \tag{2}$$

And the total reaction is as follows:

$$H_2 + \frac{1}{2}O_2 \rightarrow H_2O \tag{3}$$

Optimizing the effectiveness and operation of FCs via enhancing materials (with nanostructures) applied as FC elements is presently under consideration. For instance, the utilization of aluminum magnesium as a negative electrode component like cobalt and different materials with other formulations applied as positive electrodes such as manganese (Mn) and the use of thin layers of electrolyte [29].

Different materials and their various compounds are used to improve SOFC improvement. However, for multi-purpose materials for use in SOFC devices, further development is needed and cell's each element is better with reinforced characteristics [30]. Such issues mostly depend on the materials' operation at the scale level of scale. Therefore, the major elements of the FC package need a profound knowledge of the process science to adapt, nevertheless, the many technical issues associated with this SOFC improvement are concerned to science of materials directly [31]. For example, the material challenges associated with electrolyte inducers in terms of manufacturing process and cost can be considered.

In addition, any improvements in material properties in SOFC mainly affect chemical compatibility, electrical conductivity, thermal stability, and catalyst capacity. Moreover, the typical characteristics of such elements should include: first, interface and electrolyte should both be extremely densified to avoid gas composition. Second, cathode and anode should be adequately organized and porous structured to allow gas transfer at sites of reaction with maximum electronic and ionic conductivity of the two electrodes. In addition, from an electro-chemical perspective, the electrolyte must be strongly ionic inductor and the interfaces must be an electrical inductor next to the electrodes.

3. THE RADIAL BASIS FUNCTION NETWORK (RBF)

RBF networks are a popular kind of feed forward ANN that can be utilized in different applications. This network delivers one hidden RBF layer with a linear output layer. The main advantage if these networks is that the learning speed of the RBF networks is too fast. Consider an RBF network with input and output as $W = [w_1, w_2, \ldots, w_n]$, and $Z = [z_1, z_2, \ldots, z_n]$, respectively.

RBF unit is a neuron with several actual inputs W and one output Z calculated as:

$$Z = f(U) \tag{4}$$

$$U = \frac{W - T_\beta}{b} \tag{5}$$

where, $b \in R$ specifies the width, $T \in R^n$ defines

the center, $\cdot\beta$ determines a weighted norm and is formulated as:

$$W_\beta^2 = (\beta W)^T (\beta W) \tag{6}$$

and $f : R \to R$ defines the network activation function that is considered as:

$$f(w) = e^{-w^2} \tag{7}$$

Consequently, the RBF function defines the equation below:

$$f_k(W) = \sum_{i=1}^{h} w_{ik} e^{-\left(\frac{W - T_\beta}{b}\right)^2} \tag{8}$$

$$k = 1, 2, \ldots, M \tag{9}$$

where, $w_{ik} \in R$ and f_k represents the k^{th} weights of the output unit and network output, respectively.

The main purpose of learning the RBF network is to provide appropriate values for the units of RBF parameters and the weights of the output layer, such that the it approaches to a function that is defined by an example set, namely training set. The training process provides the best results when the value of error between the measured data and the desired data is minimum. The error value is given below:

$$E = \frac{1}{2} \sum_{j=1}^{L} \sum_{i=1}^{M} e_i^2(t) \tag{10}$$

$$e_i(t) = d_j(t) - f_i(t) \tag{11}$$

4. THE HIERARCHICAL RADIAL BASIS FUNCTION (HRBF) NETWORK

With assuming terminal instruction set (T) and a function set (F) utilized to generate a HRBF network model is defined by $S = F \cap T = [+_2, +_3, \ldots, +_N] \cup [w_1, w_2, \ldots, w_n]$, where $+_i$ defines the instructions of the non-leaf nodes (nlN) with i arguments. The instructions of the leaf nodes width no arguments are $w_1, w_2, \ldots, w_n$. The nlN output is evaluated as a model of hierarchical radial basis function network which can be seen in Fig. (1).

The $+_i$ is an original function operator including i number of inputs. Here, Gaussian RBF has been employed for the networks. The inputs number and RBF are considered equal, i.e., $n = M$. During the HRBF network tree generation process, when $+_i$ has been chosen, i numbers of randomly generated real values have been utilized for defining the connecting power between the i^{th} node and its offspring.

Furthermore, $2 \times n^2$ tunable variables α_i and β_i have been randomly generated as the variables of the RBF. The i^{th} output is achieved using Eq. (4)- Eq. (8). The HRBF network tree output has been evaluated by depth-first method from the left side. Optimal selection of the HRBF network arrangement is a nonlinear and complex problem. A proper technique for optimum choice of the network arrangement is to use metaheuristics. In this study, the provided structure is optimal-based in a new developed algorithm, which is Developed Coronavirus Herd Immunity Algorithm.

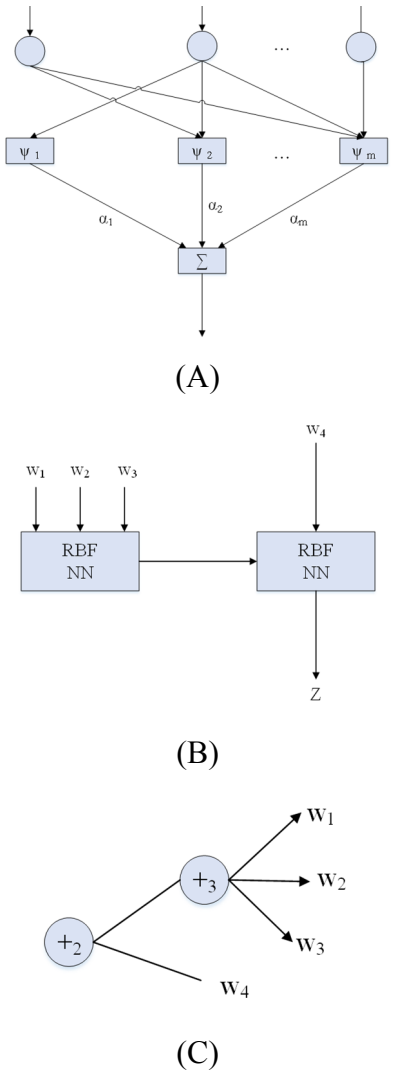

Fig. 1. (A) basic RBF network, (B) HRBF network, and (C) tree-structural HRBF network

5. DEVELOPED CORONAVIRUS HERD IMMUNITY ALGORITHM

5.1. Coronavirus herd immunity optimizer

Viruses develop and spread rapidly between people very quickly. A large population should be vaccinated to prevent the spread of the virus, but it will take some time for the vaccine to be discovered for the new virus. Therefore, until a new vaccine is discovered, the health care organizations make the following recommendations to people:

1) Infected people and those who have been in communication with them should be isolated and quarantined.
2) To prevent the spread of the virus, the principle of herd immunity is used, and thus a large part of the population must be protected to protect susceptible individuals.

5.2. Inspiration

Viruses multiply in the host body after being transmitted between people. The new virus spread many countries from Wuhan, China, in December 2019, which the World Health Organization called the epidemic of coronavirus (COVID-19). As of March 27, 2020, there were 532,279 cases in 199 countries and around the world.

Covid-19 can stay in the body for 2 to 11 days without any symptoms. Due to the fact that there is still no cure for this disease, the mortality rate of this disease is between 0.25 and 3.0%.

The spread of the disease is stopped by herd immunity, at which time a many persons in the community are immune to the disease, either by natural infection or by vaccinating. One of the methods that reduces the transmission of coronavirus and controls the spread of this disease is herd immunity because in this case higher than 65% of the population is improved from the disease. In this method, the principle of survival of the fittest (in Darwinian theory) is used.

The infected one with the corona virus in two ways:

1) When they are in close contact (less than 2 meters) with an infected person, they become infected with droplets of cough or sneezing.
2) When the surface or device is a carrier of the virus and after contact with it, the person touches their nose, eyes or mouth. Herd immunity and quarantine in the country are methods used by governments to prevent the COVID-19 epidemic until the vaccine is discovered.

A person who is infected with the corona virus can spread the virus to others. If a person has a strong immune system, he or she will defeat the virus and become immune, otherwise he or she will die. Older people have a weaker immune system or may have other illnesses such as cancer, diabetes or heart disease. As a result, older people are less likely to defeat the corona virus. According to research, the following steps are necessary to attain herd immunity:

- Many infected people transmit the virus to more people and infect them.
- Many infected people have improved and few have died.
- Over time, most people will be immune against the illness.

In the Coronavirus herd immunity optimizer, the herd immunity method is modeled. The contents of COVID-19 with the optimization context are presented in Table 1, and a set of stages is described below, and these stages are specified by CHIO:

Stage 1 initialize optimization problem and variables of CHIO in this stage. The following formula represents the objective function in the optimization problem at this stage.

$$\min_{x} f(x) \tag{12}$$

Where, x is between lb and ub. The degree of immunity of each individual or the objective

Table 1. Connection between COVID-19 and context of optimization

No	Context of COVID-19	Context of Optimization
1	Mortality rate	Reaching maximum age
2	Reproductive number	Basic reproduction rate
3	(infected, susceptible, immuned) Case	Solution
4	Social distancing	Pick random case and rely on the basic reproduction rate
5	Possibility of infection	Weak fitness value and inherit COVID-19 features
6	Transmission speed	Basic reproduction rate
7	Immunity rate	Fitness value

function of each case is determined by $f(x)$. The decision variable, or each person's gene, is denoted by x, that x is equal to $(x_1, x_2, \ldots, x_n)$, and the whole number of genes in each case expressed by n. The upper and lower bounds of gene are specified by ub_i and lb_i, That x_i is between lb_i and ub_i.

CHIO contains 4 algorithmic variables which are described below:

- The quantity of initial diseased case which starts with one item here, and expressed by C_0.
- The maximum number of iterations is indicated by Max_Itr.
- The population size is indicated by HIS.
- The problem dimensionality is expressed by n.
- CHIO also includes two main control variables, which are quantified at this stage:
- Basic reproduction rate (BR_r) is used to control CHIO operators, which is done by distribution the virus pandemic among people.
- The maximum age of people infected is determined by Max_{Age}. This variable defines the status of infected people. Infected people who reach Max_{Age} is either die or improve.

Stage 2 Create herd immunity (HI) population Primarily, CHIO creates a random set of individuals in the number of HIS. A set of created items according to the following formula is saved as a 2D $n \times HIS$ matrix in the HI population.

$$HIP = \begin{bmatrix} x_1^1 & x_2^1 & \cdots & x_n^1 \\ x_1^2 & x_2^2 & \cdots & x_n^2 \\ \vdots & \vdots & \cdots & \vdots \\ x_1^{HIS} & x_2^{HIS} & \cdots & x_n^{HIS} \end{bmatrix} \quad (13)$$

In the above formula, each row j specifies a case x^j, that is obtained according to the following formula: $x_i^j = lb_i + (ub_i - lb_i) \times U(0,1), \forall i = 1,2,\ldots,n.$ as mentioned earlier, the objective function for each case is obtained according to Formula 1. the status vector (S) for wholly cases in HI population is started by infected case (1) or sensitive case (0). Also, the quantity of infected cases (one) in S is started as many as C_0 by chance.

Stage 3 Coronavirus HI development, which is the CHIO's key development loop. Case (x^j) related gene (x_i^j) is remain constant or is obtained under the influence of social distancing using the three laws according to BR_r:

$$x_i^j(t+1) \leftarrow \begin{cases} x_i^j(t) & r \geq BR_r \\ C\left(x_i^j(t)\right) & r < \frac{1}{3} \times BR_r \text{ .//infected case} \\ N\left(x_i^j(t)\right) & r < \frac{2}{3} \times BR_r \text{ .//susceptible case} \\ R\left(x_i^j(t)\right) & r < BR_r \text{ .//immuned case} \end{cases} \quad (14)$$

Here r creates a random amount between 0 and 1. The rules have been stated in the following:

Infected item: In the range of $r \in \left[\frac{0,1}{3BR_r}\right]$, the new gene amount of $x_i^j(t+1)$ is impacted by some social spacing and that is attained by the dissimilarity among present one and the one attained from an infected item x^c for example

$$x_i^j(t=1) = C\left(x_i^j(t)\right) \quad (15)$$

Here

$$C\left(x_i^j(t)\right) = x_i^j(t) + r \times \left(x_i^j(t) - x_i^c(t)\right) \quad (16)$$

The amount of $x_i^c(t)$ has been chosen from some infected case x^c based on the status vector (S), thus,

$$c = (i \mid S_i = 1)$$

Susceptible item: defined in $r \in \left[\frac{1}{3}BR_r, \frac{2}{3}BR_r\right)$, the new gene value of $x_i^j(t+1)$ is impacted by some social spacing and that is attained by the dissimilarity among present one and the one attained from a susceptible item x^v for example

$$x_i^j(t+1) = N\left(x_i^j(t)\right) \quad (17)$$

Here

$$N\left(x_i^j(t)\right) = x_i^j(t) + r \times \left(x_i^j(t) - x_i^v(t)\right) \quad (18)$$

The amount of $x_i^v(t)$ is randomly extent from some susceptible case x^v based on the status vector (S), thus, $v = (i \mid S_i = 0)$.

Immuned item: In the range of $r = \left[\frac{2}{3}BR_r, BR_r\right)$, the new gene amount of $x_i^j(t+1)$ is impacted by several social spacing and that is attained by the dissimilarity among the present one and the one attained from an immuned item x^z for example

$$x_i^j(t+1) = R(x_i^j(t)$$

Here

$$R\left(x_i^j(t)\right)=x_i^j(t)+r\times\left(x_i^j(t)-x_i^v(t)\right) \quad (20)$$

The amount of x_i^z (t) is extent from the finest immuned item x^z according to the status vector (S) for example:

$$f\left(x^z\right)=arg_{j\sim}min_{[k|S_k=2]}f\left(x^j\right).$$

The next stage is to update HI population. The immunity amount $f\left(x^j(t+1)\right)$ of each created item $x^j(t+1)$ is designed and the present case $x^j(t)$ is changed by the created item $x^j(t+1)$, if improved, such as $f\left(x^j(t+1)\right)<f\left(x^j(t)\right)$. If $S_j=1$ the age amount A_j is increased by one.

The following formula is used to update the status vector (S_j).

$$S_j\leftarrow\begin{cases}1 & f\left(x^j(t+1)\right)<\dfrac{f(x)^j(t+1)}{\Delta f(x)}\wedge \\ & S_j=0\wedge is\_Corona\left(x^j(t+1)\right)\\ 2 & f\left(x^j(t+1)\right)>\dfrac{f(x)^j(t+1)}{\Delta f(x)}\wedge \\ & S_j=1\end{cases} \quad (21)$$

A binary value equal to 1 is denoted by $is\_Corona\left(x^j(t+1)\right)$ while the new case $x^j(t+1)$ has taken a amount from some infected one. The $\Delta f(x)$ is the average amount of the population immune rates for example $\frac{\sum_{j=1}^{HIS}f(x_i)}{HIS}$. In case the immunity rate of new individual is more proper than the mean population immunity, the degree of immunity of individuals is obtained according to social distance. As a result, we will have a more secure population. When the newly produced population is sufficiently safe against the epidemic, we will obtain the HI threshold.

Stage 5 is Fatalness cases. If the rate of immunity $f\left(x^j(t+1)\right)$ of the present infected person ($S_j=1$) cannot recover for a definite iterations' number as quantified using the variable Max_Age (i.e., $A_j\geq Max\_Age$) so this person is considered died. Then, to variegate the present population and escape local optimization, it is recreated over again by $x_i^j(t+1)=lb_i+\left(ub_i-lb_i\right)\times U(0,1)$, $\forall i=1,2,\ldots,n.$

Stage 6 Stop condition CHIO repeats phases three through six until the termination condition is happened. The termination condition usually depends on the maximum number of repetitions. After reaching the termination criterion, the whole number of safe cases prevails over the population and the infected cases vanish.

5.3. Developed Coronavirus Herd Immunity Algorithm (DCHIA)

Although, the original Coronavirus Herd Immunity (CHI) optimizer is a recent metaheuristic optimizer, it delivers effective achievements for the considered problems [32], it can have some problems such as achieving low convergence speed and local optimization which can be modified by some improvements. Here, a recent advanced version of CHI algorithm is suggested to provide an effective version of this algorithm to use as an optimal tool to model parameters identification.

One mechanism is to use the opposition-based learning (OBL) mechanism [33]. This mechanism is a mechanism to increase the exploration ability of the metaheuristics [34]. This mechanism generates a complement value for the candidate to provide pairs of initial populations. In the new population, the pairs compete with each other and the better one is selected as the new candidate which is analyzed by performing the two pairs to the objective function [35]. This new candidate can be the original candidate or the complement one. The complement value of each candidate can be calculated as follows:

$$x_i^{j,new}(t)=x_i^{j,max}(t)+x_i^{j,min}(t)-x_i^j(t) \quad (22)$$

where, $x_i^{j,new}(t)$ defines the opposite position of $x_i^j(t)$, and $x_i^{j,min}(t)$ describe the lower boundary and $x_i^{j,max}(t)$ is the higher boundary for the solution.

In this study, 40% of the initial population has been achieved by this mechanism. The next advancement is to use the chaos theory. Using chaos theory, we can provide results with higher convergence speed. The method generates pseudo-random candidates which improve the speed of the algorithm convergence. Different types of Chaos mechanisms have been introduced [36]. Logistic map is one of the popular types of these mechanisms. By updating random parameter r as pseudo-random variable, the updated parameters has been obtained as given below:

$$r(i+1)=\beta\times r(i)\times\left(1-r(i)\right) \quad (23)$$

where, β describes the control parameter in the

range [0, 4] (here, $\beta = 3$) [37], and $r(0)$ specifies a random amount between 0 and 1.

5.4. Algorithm validation

This section is about validation of the proposed Developed Coronavirus Herd Immunity Algorithm. The computer validation is implemented on MATLAB R2018b environment. During the validation, the control parameters are firstly defined for evaluation and then, some of the standard benchmark functions have been introduced for using in the evaluation. Afterward, researches of the studied functions are executed. The achievements of the optimizer are then put in comparison with some latest algorithms to indicate its effectiveness. The analyzed algorithms are Chimp optimization algorithm (COA) [38], Locust Swarm Optimizer (LS) [39], Emperor Penguin Optimization algorithm (EPOA) [40], and original Coronavirus Herd Immunity Algorithm [32]. Table 2 displays the utilized control parameters for the studied algorithms.

The maximum iteration and the population size for all algorithms containing the suggested Developed Coronavirus Herd Immunity Algorithm are set 50 and 200, respectively. Table 3 indicates the employed benchmark functions for validation and their constraint, and optimal value.

The optimizers were independently implemented 35 times on each one of the test functions to bring authentic achievements. To verify the ability of the proposed Developed Coronavirus Herd Immunity Algorithm, four measurement indicators have been utilized. The indicators include average amount, lowest (min) and highest (max) values, and the value of standard deviation of the algorithms' run during 35 times implementation. Table 4 states the results of comparison among the suggested Developed Coronavirus Herd Immunity optimizer and some state of the art algorithms.

It can be observed from Table 4 that the achieved amount for values of max, min, and average for the proposed method are the smallest in the proposed Developed Coronavirus Herd Immunity Algorithm. So, due to the minimization nature of the introduced benchmark functions, the proposed method provides the best results in terms of accuracy. Also, with a glance on the standard

Table 2. Utilized control parameters for the studied algorithms

Algorithm	Parameter	Value
Chimp optimization algorithm (COA) [38]	r_1 and r_2	Random
	m	Chaotic
Locust Swarm Optimization (LS) [39]	F	0.6
	L	1
	g	20
	$\vec{A}$	[-1.5, 1.5]
	Temperature value (T')	[1, 1000]
Emperor penguin optimizer (EPOA) [40]	M	2
	f	[2, 3]
	S	[0, 1.5]
	l	[1.5, 2]

Table 3. Employed benchmark functions for validation and their constraint, and optimal value

Type	Function	Formula	Dimension	Range	F_{min}
Unimodal	Sphere	$F_1(x) = \sum_{i=1}^{n} x_i^2$	30	[-100,100]	0
	Schwefel2.22	$F_2(x) = \sum_{i=1}^{n} \lvert X_i \rvert + \prod_{i=1}^{n} \lvert x_i \rvert$	30	[-10,10]	0
Multimodal Original Functions	Rosenbrock's	$F_3(x) = \sum_{i=1}^{n-1} [100(x_{i+1} - x_i^2)^2 + (x_i - 1)^2]$	30	[-30,30]	0
	Quartic	$F_4(x) = \sum_{i=1}^{n} i x_i^4 + random[0,1)$	30	[-128,128]	0

Table 4. The results of comparison among the suggested DCHIA and some latest optimizers

Metaheuristics / Function	COA [38]		LS [39]		EPOA [40]	
	Average	SD	Average	STD	Average	STD
F1	10.1264e-1	13.2648e-1	13.3817e-2	17.3729e-2	14.9471e-3	25.6447e-3
F2	16.6647e-2	24.0413e-2	20.3648e-2	25.3482e-2	20.8594e-2	28.2081e-2
F3	18.3614	17.6379	15.2258	12.7464	9.8294	6.9647
F4	1.328e-4	1.0098	1.0072	0.068	0.0052	0.0042
Metaheuristics / Function	CHI [32]			DCHIA		
	Average		STD	Average	STD	
F1	26.3925e-4		15.3251e-5	10.2374e-6	18.3617e-6	
F2	23.2574 e-2		15.4341e-3	16.6222e-3	27.8507-3	
F3	6.0157		5.9246	3.6274	2.0367	
F4	0.0098		0.0083	0.0076	0.0053	

deviation value, it is clear that this value for all of the function for the proposed Developed Coronavirus Herd Immunity Algorithm is the lowest amount among the others. The lowest amount of standard deviation for this optimizer is a prove for its higher precision, i.e., the algorithms' higher reliability among the other compared algorithms.

6. METHODOLOGY

6.1. The method of optimizing HRBF using DCHIA

As can be seen, the suggested Developed Coronavirus Herd Immunity Algorithm provides efficient results for the analyzed studied cases. Therefore, we aimed to use this technique for optimizing the HRBF structure. The main learning process for optimal HRBF network construction based on Developed Coronavirus Algorithm is given in the following.

1) Initializing the population with random candidates (including the parameters of the HRBF network trees)
2) Optimal parameters selection based on Developed Coronavirus Algorithm
3) If termination condition has been reached, go to (4), Else, go to (2)
4) The optimal parameters have been achieved by the Developed Coronavirus Optimizer. The model architecture of HRBF network has been determined in this phase and the optimum arrangement of the tree has been established.
5) If the termination condition has been reached, or there are not better results, go to (6), Else, go to (4).
6) If a promising achievement is achieved, the algorithm has been terminated; Else, go to (2).

6.2. Optimal Modeling of SOFC based on DCHIA-HRBF

During the simulation of the SOFC stack, it is determined that the relation between the output voltage of the stack (V) and the current density (I) can be affected by different operating parameters, like H_2 and O_2 flow rates, cell's temperature, and the H_2 and O_2 pressures. Although, because of existing a lot of operating variables, there is no perfect empirical database for SOFCs under different operational conditions [41].

Still now, there is no comprehensive methodology to integrate all of these operating variables. In this study, we used the proposed *DCHIA-HRBF* for modeling the system with higher accuracy, however, it is not an exception which is due to the systems' complexity with several variables. One significant operating variable which has a high impact on the SOFCs is temperature. The current density is a proper variable for investigating the impact of different temperatures on the output voltage. This variable selected by the temperature of fuel cell and uncontrollable load as variables.

Various methods have been introduced for nonlinear systems identification. This study considers a two-input, one-output Blackbox for system identification of the SOFCs, such that:

$$V_{i+1} = f\left[V_i, V_{i-1}, \ldots, V_{i-n}, I_i, I_{i-1}, \ldots, I_{i-m}, T_i\right] \tag{24}$$

By considering the inputs (i.e., $I_i, I_{i-1}, \ldots, I_{i-m}, T_i$) and the output (i.e., $V_i, V_{i-1}, \ldots, V_{i-n}$), the main construction of the system can be shown by Fig. (2).

Tapped delay line (TDL) extracts the output data from the system within the delay line as seen in Fig. (2). The major target here is to provide a technique based on DCHIA-HRBF technique to identify Eq. (24). The method includes three main stages. The firs one is to pre-process the input training data. The second stage is to use the pre-processed data to train and design the proposed DCHIA-HRBF model. Finally, the last stage is to use the designed model for new input data prediction.

7. SIMULATION RESULTS

7.1. Pre-processing the data

In the present research, we utilized a model from [42] to provide a proper dataset for training the DCHIA-HRBF model. The simulation contains two clusters of cell voltage and current density data under 1073.15 K and 1273.15 K to train the data. Both of the group has 699 data pairs. The operational variables of the FC including temperatures and stack current density (0–700 mA cm−2) are changeable. The range of the operational variables of the FC is indicated in Table 5.

To pre-process the input data to provide a proper training, we need to normalize the scale all of the input data to a definite range. This range is usually is between 0 and 1. Several methods are introduced for normalizing the data [43]. Here, Linear Scaling methodology has been utilized for scaling current density, cell voltage, and temperature between 0 and 1. By considering z as an input data, the Linear Scaling can be defined as follows:

$$z' = \frac{z_j - z_{min}}{z_{max} - z_{min}} \tag{25}$$

where, z_{min} and z_{max} stand for the lowest and the highest amount of the data.

7.2. Parameter selection of the suggested DCHIA-HRBF

For speeding up the identification process, we should prune some of the useless parameters. As mentioned before, the proposed *DCHIA-HRBF* network includes two inputs (temperature and current density), one output (voltage), and 4 nodes for hidden layer.

7.3. The Main Objective

The parameters of the HRBF network have been assumed as the decision parameters herein. The decision variables should be optimally selected by the Developed Coronavirus Herd Immunity Algorithm to provide an optimized configuration for the HRBF network. Therefore, the population here includes the Gaussian function (GF)'s width

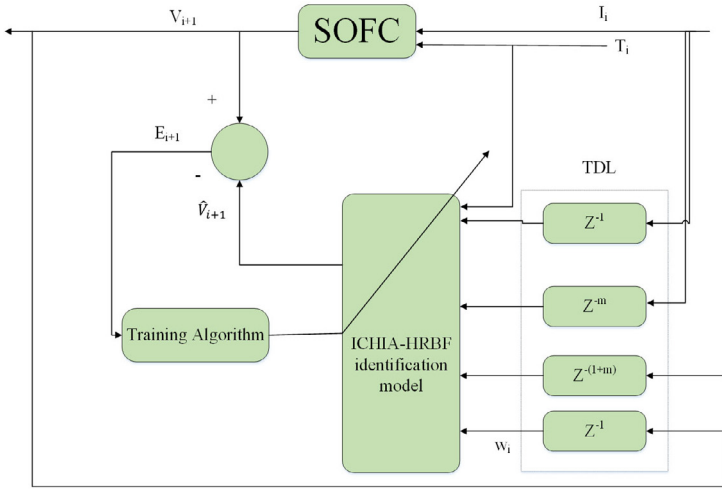

Fig. 2. The main configuration of the proposed DCHIA-HRBF

Table 5. The range of the operational variables of the FC

Operational variables	Lower Range	Upper Range	Unit
Temperature	873.15	1273.15	Kelvin (K)
Current density	0	700	mA/cm^2

and center and the weights of the output. So, the population definition in HRBF network is as follows:

$$p = \begin{bmatrix} a_1, a_2, a_3, a_4, c_{11}, c_{12}, c_{13}, c_{14}, \\ c_{21}, c_{22}, c_{23}, c_{2,4}, \alpha_1, \alpha_2, \alpha_3, \alpha_4 \end{bmatrix} \quad (26)$$

Therefore, the population includes 16 parameters for each candidate vector, where, 4 widths and 4 centers for the RBF network's hidden unit and 4 weights are considered for connection. The constraints for the parameters are as follows:

$$\begin{aligned} &0.1 \le a_i \le 3 \\ &-3 \le c_{ji} \le 3 \\ &-1 \le \alpha_i \le 1 \end{aligned} \quad (27)$$

$$i = 1,2,3,4; j = 1,2 \quad (28)$$

The solution candidates (decision variables) of the generation have been assessed by a performance index (PI). This study uses HRBF network has been employed to model the SOFC stack. The main objective function for this study is formulated below

$$PI = \frac{1}{50 \times \sum_{j=1}^{M} |e(j)|} \quad (29)$$

here, M refers to the samples number for the experimental information, and $e(j)$ describes the error amount between the output of model and empirical output. The major concept is to lessen this index using the Developed Coronavirus Herd Immunity Algorithm.

In the classic methods, to optimize the above-mentioned performance index, the decision variables are achieved by using gradient descent learning algorithm. In this study, Developed Coronavirus Herd Immunity Algorithm has been used for this purpose. Table 6 indicates the optimal selected decision variables including the outputted weights and the GF's widths and centers.

As mentioned, the optimal parameter values have been achieved by minimizing Eq. (29). Fig. (3) shows the optimal value that is achieved by the proposed method. As can be observed from Fig. (3), the best cost for the performance index is 119.442.

Table 6. Optimal selected decision variables of the network

Parameter	Value	Parameter	Value
a_1	1.856	c_{11}	0.255
a_2	1.439	c_{12}	-0.763
a_3	2.615	c_{13}	-0.446
a_4	2.408	c_{14}	-0.259
α_1	-0.556	c_{21}	-1.437
α_2	0.772	c_{22}	1.565
α_3	0.709	c_{23}	-2.962
α_4	0.591	c_{24}	-0.101

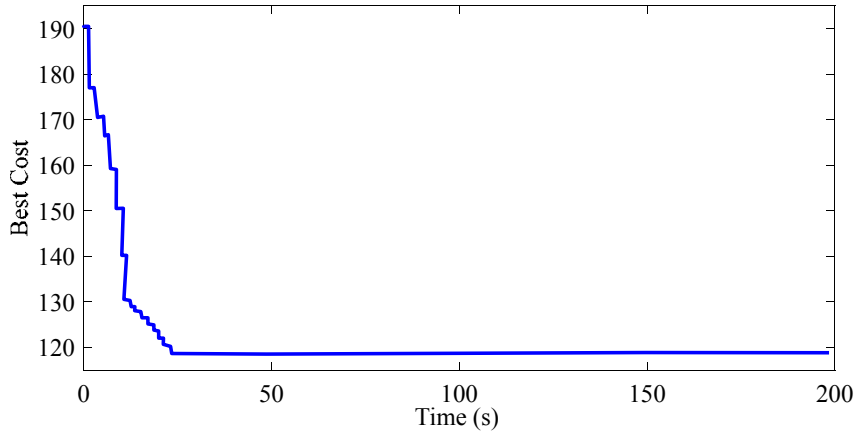

Fig. 3. The convergence value curve of the best cost candidates

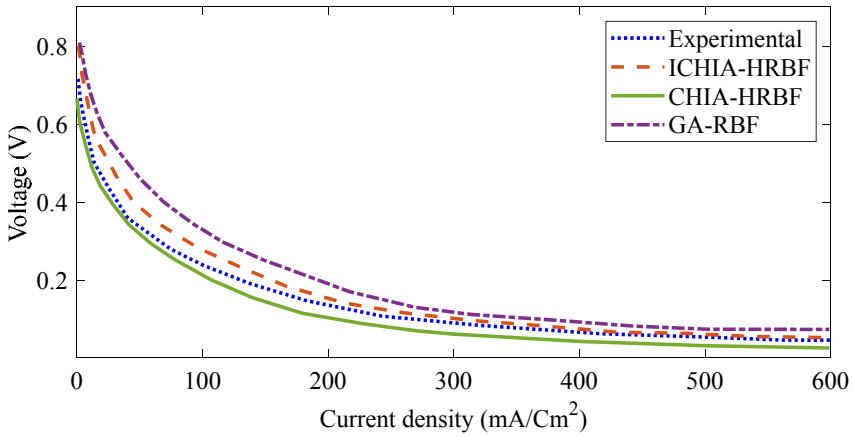

Fig. 4. Current-voltage curve validation for the achieved method based on DCHIA-HRBF and other comparative algorithms for T=873.15 K

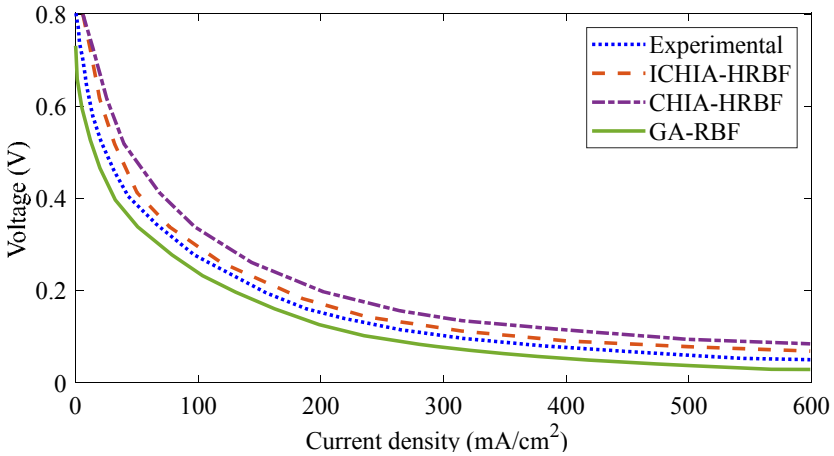

Fig. 5. Current-voltage curve validation for the achieved method based on DCHIA-HRBF and other comparative algorithms for T=1223.15 K

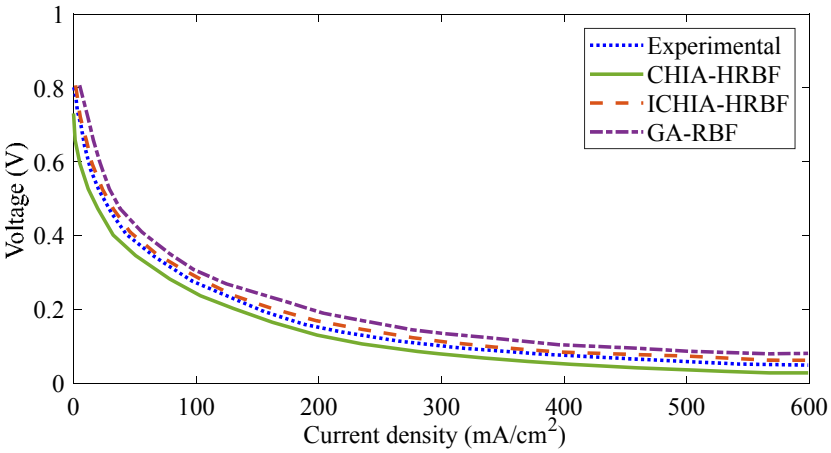

Fig. 6. Current-voltage curve validation for the achieved method based on DCHIA-HRBF and other comparative algorithms for T=1173.15 K

Fig. (4-6) show the current-voltage curve for the optimized method based on the trained data for $T = 1173.15 K$ according to the suggested DCHIA-HRBF comparing with GA-RBF [41], and the original CHI-HRBF for confirmation with the experimental data.

Based on Fig. (4-6), the suggested DCHIA-HRBF model provided the best confirmation with the experimental data during different Temperatures. In the next step, we utilized the DCHIA-HRBF network for data prediction. Here, after performing the training step, DCHIA-HRBF network has been modeled and prepared for using in prediction. In the present study, we also used the test data from [42]. The prediction analysis is also performed by considering the $873.15\ K$ with current density between 0 and 600 mA cm^{-2}. To verify the results of the predicted output, it is confirmed by experimental data. The evaluation is shown in Fig. (4-6).

8. CONCLUSIONS

The current paper suggests a new methodology for Blackbox system identification of the solid oxide fuel cells (SOFCs). The approach has been was developed by a new developed version of Radial Basis Function (RBF), called Hierarchical RBF (HRBF) to provide better results. To provide higher efficiency for the proposed HRBF, its structure was optimized by a new developed metaheuristic, called Developed Coronavirus Herd Immunity Algorithm. The proposed model named DCHIA-HRBF and after designing the model based on training data, its efficiency was confirmed with comparison of some other latest approaches. The approach was also verified by doing a validation by the empirical data. The achievements indicated that the proposed DCHIA-HRBF provides high efficiency as an identification and prediction tool for the SOFCs.

REFERENCES

1. Cao, Y., et al., *Experimental modeling of PEM fuel cells using a new improved seagull optimization algorithm.* Energy Reports, 2019. **5**: p. 1616-1625.
2. Akbary, P., et al., *Extracting appropriate nodal marginal prices for all types of committed reserve.* Computational Economics, 2019. **53**(1): p. 1-26.
3. Bagheri, M., et al. *A novel wind power forecasting based feature selection and hybrid forecast engine bundled with honey bee mating optimization*. in *2018 IEEE International Conference on Environment and Electrical Engineering and 2018 IEEE Industrial and Commercial Power Systems Europe (EEEIC/I&CPS Europe)*. 2018. IEEE.
4. Cai, W., et al., *Optimal bidding and offering strategies of compressed air energy storage: A hybrid robust-stochastic approach.* Renewable Energy, 2019. **143**: p. 1-8.
5. Ye, H., et al., *High step-up interleaved dc/dc converter with high efficiency.* Energy Sources, Part A: Recovery, Utilization, and Environmental Effects, 2020: p. 1-20.
6. Yu, D. and N. Ghadimi, *Reliability constraint stochastic UC by considering the correlation of random variables with Copula theory.* IET Renewable Power Generation, 2019. **13**(14): p. 2587-2593.
7. Dehghani, M., et al., *Blockchain-based securing of data exchange in a power transmission system considering congestion management and social welfare.* Sustainability, 2021. **13**(1): p. 90.
8. Ebrahimian, H., et al., *The price prediction for the energy market based on a new method.* Economic research-Ekonomska istraživanja, 2018. **31**(1): p. 313-337.
9. Cao, Y., et al., *Multi-objective optimization of a PEMFC based CCHP system by meta-heuristics.* Energy Reports, 2019.
10. Eslami, M., et al., *A New Formulation to Reduce the Number of Variables and Constraints to Expedite SCUC in Bulky Power Systems.* Proceedings of the National Academy of Sciences, India Section A: Physical Sciences, 2018: p. 1-11.
11. Fan, X., et al., *High voltage gain DC/DC converter using coupled inductor and VM techniques.* IEEE Access, 2020. **8**: p. 131975-131987.
12. Firouz, M.H. and N. Ghadimi, *Concordant controllers based on FACTS and FPSS for solving wide-area in multi-machine power system.* Journal of Intelligent & Fuzzy Systems, 2016. **30**(2): p. 845-859.
13. Guo, Y., et al., *An optimal configuration for a battery and PEM fuel cell-based hybrid energy system using developed Krill herd optimization algorithm for locomotive application.* Energy Reports, 2020. **6**: p. 885-894.
14. Ghadimi, N., *An adaptive neuro-fuzzy inference system for islanding detection in wind turbine as distributed generation.* Complexity, 2015. **21**(1): p. 10-20.
15. Yuan, Z., et al., *Probabilistic decomposition-based security constrained transmission expansion planning incorporating distributed series reactor.* IET Generation, Transmission & Distribution, 2020. **14**(17): p. 3478-3487.
16. Meng, Q., et al., *A single-phase transformer-less grid-tied inverter based on switched capacitor for PV application.* Journal of Control, Automation and Electrical Systems, 2020. **31**(1): p. 257-270.
17. Gheydi, et al., *Planning in microgrids with conservation of voltage reduction.* IEEE Systems Journal, 2016. **12**(3): p. 2782-2790.
18. Hosseini Firouz, et al., *Optimal preventive maintenance policy for electric power distribution systems based on the fuzzy AHP methods.* Complexity, 2016. **21**(6): p. 70-88.
19. Yuan, Z., et al., *A new technique for optimal estimation of the circuit-based PEMFCs using developed Sunflower Optimization Algorithm.* Energy Reports, 2020. **6**: p. 662-671.
20. Yu, D., et al., *System identification of PEM fuel cells using an improved Elman neural network and a new hybrid optimization algorithm.* Energy Reports, 2019. **5**: p. 1365-1374.
21. Xiong, G., et al., *A simplified competitive swarm optimizer for parameter identification of solid oxide fuel cells.* Energy

Conversion and Management, 2020. **203**: p. 112204.
22. Alhumade, H., et al., *Optimal Parameter Estimation Methodology of Solid Oxide Fuel Cell Using Modern Optimization.* Mathematics, 2021. **9**(9): p. 1066.
23. Yang, B., et al., *Extreme learning machine based meta-heuristic algorithms for parameter extraction of solid oxide fuel cells.* Applied Energy, 2021. **303**: p. 117630.
24. Ba, S., D. Xia, and E.M. Gibbons, *Model identification and strategy application for Solid Oxide Fuel Cell using Rotor Hopfield Neural Network based on a novel optimization method.* International Journal of Hydrogen Energy, 2020. **45**(51): p. 27694-27704.
25. Jia, H. and B. Taheri, *Model identification of Solid Oxide Fuel Cell using hybrid Elman Neural Network/Quantum Pathfinder algorithm.* Energy Reports, 2021. **7**: p. 3328-3337.
26. Fei, X., et al., *Optimal configuration and energy management for combined solar chimney, solid oxide electrolysis, and fuel cell: a case study in Iran.* Energy Sources, Part A: Recovery, Utilization, and Environmental Effects, 2019: p. 1-21.
27. Tian, M.-W., et al., *New optimal design for a hybrid solar chimney, solid oxide electrolysis and fuel cell based on improved deer hunting optimization algorithm.* Journal of Cleaner Production, 2020. **249**: p. 119414.
28. Zhi, Y., et al., *New approaches for regulation of solid oxide fuel cell using dynamic condition approximation and STATCOM.* International Transactions on Electrical Energy Systems: p. e12756.
29. Ramezani, M., et al., *A new optimal energy management strategy based on improved multi-objective antlion optimization algorithm: applications in smart home.* SN Applied Sciences, 2020. **2**(12): p. 1-17.
30. Yang, Z., et al., *Model parameter estimation of the PEMFCs using improved Barnacles Mating Optimization algorithm.* Energy, 2020. **212**: p. 118738.
31. Yanda, L., Z. Yuwei, and N. Razmjooy, *Optimal arrangement of a micro-CHP system in the presence of fuel cell-heat pump based on metaheuristics.* International Journal of Ambient Energy, 2020: p. 1-12.
32. Al-Betar, M.A., et al., *Coronavirus herd immunity optimizer (CHIO).* Neural Computing and Applications, 2021. **33**(10): p. 5011-5042.
33. Tizhoosh, H.R. *Opposition-based learning: a new scheme for machine intelligence.* in *International conference on computational intelligence for modelling, control and automation and international conference on intelligent agents, web technologies and internet commerce (CIMCA-IAWTIC'06)*. 2005. IEEE.
34. Ramezani, M., D. Bahmanyar, and N. Razmjooy, *A New Improved Model of Marine Predator Algorithm for Optimization Problems.* Arabian Journal for Science and Engineering, 2021: p. 1-24.
35. Wang, Z., et al., *A new configuration of autonomous CHP system based on improved version of marine predators algorithm: A case study.* International Transactions on Electrical Energy Systems: p. e12806.
36. Razmjooy, N., M. Khalilpour, and M. Ramezani, *A new meta-heuristic optimization algorithm inspired by FIFA world cup competitions: theory and its application in PID designing for AVR system.* Journal of Control, Automation and Electrical Systems, 2016. **27**(4): p. 419-440.
37. Yang, D., Z. Liu, and J. Zhou, *Chaos optimization algorithms based on chaotic maps with different probability distribution and search speed for global optimization.* Communications in Nonlinear Science and Numerical Simulation, 2014. **19**(4): p. 1229-1246.
38. Khishe, M. and M.R. Mosavi, *Chimp optimization algorithm.* Expert Systems with Applications, 2020: p. 113338.
39. Cuevas, E., F. Fausto, and A. González, *The Locust Swarm Optimization Algorithm*, in *New Advancements in Swarm Algorithms: Operators and Applications*. 2020, Springer. p. 139-159.
40. Dhiman, G. and V. Kumar, *Emperor penguin optimizer: A bio-inspired algorithm for engineering problems.* Knowledge-Based Systems, 2018. **159**: p. 20-50.
41. Wu, X.-J., et al., *Modeling a SOFC stack based on GA-RBF neural networks identification.* Journal of Power Sources, 2007. **167**(1): p. 145-150.
42. Calise, F., et al., *Simulation and exergy analysis of a hybrid solid oxide fuel cell (SOFC)–gas turbine system.* Energy, 2006. **31**(15): p. 3278-3299.
43. Liu, X., et al., *Normalization methods for the analysis of unbalanced transcriptome data: a review.* Frontiers in bioengineering and biotechnology, 2019. **7**: p. 358.